

Interaction of a Bose-Einstein condensate with a surface: perturbative S-matrix approach

Jürgen Schiefele and Carsten Henkel

Universität Potsdam, Institut für Physik und Astronomie, Karl-Liebknecht-Str. 24/25,

14 476 Potsdam, Germany

E-mail: Juergen.Schiefele@physik.uni-potsdam.de

Abstract

We derive an expression for the collective Casimir-Polder interaction of a trapped gas of condensed bosons with a plane surface through the coupling of the condensate atoms with the electromagnetic field. A systematic perturbation theory is developed based on a diagrammatic expansion of the electromagnetic self-energy. In the leading order, the result for the interaction-energy is proportional to the number of atoms in the condensate mode. At this order, atom-atom interactions and recoil effects lead to corrections compared to the single-atom theory, through shifts of the atomic transition energies. We also discuss the impact of the spatial delocalization of the condensate mode.

1 Introduction

It is well known from cavity quantum electrodynamics (cavity QED) that the energy levels and lifetimes of the electronic states of an atom placed near a macroscopic body are shifted from their free-space values [1,2]. This effect can be understood from the modification the body imposes on the vacuum field modes which lead, for example, to a position-dependent change in the Lamb shift. The resulting (van der Waals or Casimir-Polder) force between the atom and the macroscopic body has been shown to match the predictions of QED in several experiments [3–7].

As cavity QED effects often do not require a relativistic treatment of the electronic or atomic motion, the techniques traditionally employed are lent from non-relativistic QED: a mode expansion of the electromagnetic field and a first quantized theory for the remaining (atomic) part of the system [8]. Instead of working with mode expansions adapted to the presence of a body, there is another approach making use of the fluctuation-dissipation theorem [9, 10]: the level shift is cast in a form involving generalized susceptibilities from linear response theory, the (retarded) Green functions. The influence of the surface is then encoded in the appropriate scattering amplitudes of the body, e.g., reflection coefficients for a planar interface. This makes the approach applicable to very general descriptions of the surface material, including absorption and dispersion. Another advantage of the formalism lies in the fact that renormalization gets simplified, as the (divergent) free-space part of the Lamb shift is easily isolated from the surface-dependent contributions, the latter being finite.

In the present paper, we are interested in the shift of the collective energy levels of an N -atom system due to the presence of a nearby surface. A theory that has to account for the quantum statistical character of atoms is conveniently formulated in terms of second-quantized atom field operators. We follow the standard procedure for perturbation theory, which offers a pictorial representation in terms of Feynman diagrams and permits us to calculate the elements of the electromagnetic self-energy, approximating them

with the Dyson series [11]. For our purposes, the theory has to deal with a confined atomic system in a trap (including inter-atomic interactions), and the interaction with the electromagnetic field is the relevant perturbation. While much of the literature on Bose-Einstein condensates (BECs) in an external potential deals mainly with the collective properties of atoms in their electronic ground state, a quantum field theory of ultra-cold atoms interacting with photons was formulated in [12, 13]. We build on this approach and merge it with the linear response techniques for electromagnetic field fluctuations near a surface. In the present paper, we consider the atom-light interaction up to second order, which is the first non-vanishing contribution. We find under quite general circumstances the atom-surface interaction energy and demonstrate that it does not reduce to an integral over the density distribution of trapped (ground state) atoms. The propagation in the excited state, although only virtually, connects ground state correlation functions at different space-time points. This leads to a recoil shift of the atomic polarizability, in addition to the familiar density shifts due to the atom-atom interaction. For the atomic ensemble, we consider two simple examples: firstly, an interacting BEC at temperatures well below the critical temperature, where we consider only a single mode of the atomic field with macroscopic occupation. Our second example is the ideal Bose gas at nonzero temperature that can be essentially characterized analytically. Both systems are held in harmonic traps centered near the surface. We develop in this paper the main methods, check that several limiting cases are recovered and discuss the two examples above in some detail. The aim for future publications is to generalize this approach in two respects: on the cavity-QED side of the problem, to push the atom-field interaction to higher orders and, on the BEC side, to take into account low-lying collective states of the interacting atomic ensemble like Bogoliubov quasi-particles.

The paper is organized as follows: In section 2, we describe the interaction of the atomic system and the electromagnetic field, in a form involving second quantized operators for atoms as well as for the field. In section 3, we calculate a general expression for the energy shift of the atomic ensemble due to the interaction with the electromagnetic (e.m.) field by evaluating the first non-vanishing term in the Dyson expansion of the S -matrix. The result thus obtained involves the Feynman propagator for the e.m. field in the presence of a surface which is introduced in section 4.1. Atomic propagators are calculated in section 4.2.1 and section 4.2.2 for an interacting BEC (zero temperature) and an ideal gas (nonzero temperature), respectively. The results of section 2 to section 4 are then used to calculate the atom-surface interaction of these two examples (section 5 and section 6). We cross-check our calculations against existing results in section 5.4, by re-deriving the Casimir-Polder potential for a single perfectly localized atom.

Our units are such that $\hbar = k_B = 1$, the speed of light c and the atomic mass M are kept for the ease of reading.

2 Quantum field theory of atoms and photons

We consider N identical atoms in a trap above a flat surface. The surface is taken to lie in the xy -plane, the center of the trap is located a distance d from the surface in the half-space $z > 0$. The atoms are treated in the electric dipole approximation with an electric ground state $|g\rangle$ and excited states $|e\rangle$. The extension of this model to more realistic atoms is straightforward by summing the contributions of all excited states in the calculation of the ground state shift.

Apart from possible inter-atomic interactions, the atoms interact with the electromagnetic field via a $\boldsymbol{\mu} \cdot \mathbf{E}$ interaction term, where the dipole operator has transition matrix elements $\boldsymbol{\mu}^{ge} = \langle g | \mathbf{d} | e \rangle$. (For a comparison between the minimal coupling Hamiltonian and $\boldsymbol{\mu} \cdot \mathbf{E}$ interaction, see [14, 15].) The interaction between the atomic system and the surface originates in this atom-field coupling: the surface contains sources that radiate a field, and it imposes boundary conditions on both the intrinsic field fluctuations and the field radiated by the atom. The relevant correlation functions of \mathbf{E} near the surface will be dealt with in section 4.1.

As in [12], we will work with a Hamiltonian that describes the atomic degrees of freedom (as well as the

electric field) in second quantization i.e., a quantum field theory of atoms interacting with photons. The operators $\Psi_g(\mathbf{r})$ and $\Psi_e(\mathbf{r})$ describe the annihilation of an excited-state or ground state atom at location \mathbf{r} .

As we want to treat the influence of the electromagnetic coupling as a perturbation to the atomic system, we split the total Hamiltonian as follows:

$$H = H_A + H_{AF} + H_F \quad (2.1)$$

Here, H_F is the Hamiltonian for the unperturbed field in the presence of the surface, H_{AF} contains the atom-field interaction, and the Hamiltonian H_A describes the trapped atoms. The atomic operators in an interaction-picture with respect to H_{AF} then have the general form

$$\Psi_g(x) = \sum_{\mathbf{n}} \Phi_{\mathbf{n}}(\mathbf{r}) \hat{g}_{\mathbf{n}}(t), \quad (2.2)$$

$$\Psi_e(x) = \int \frac{d^3q}{(2\pi)^{3/2}} \exp(i\mathbf{q}\cdot\mathbf{r}) \hat{e}_{\mathbf{q}}(t). \quad (2.3)$$

where the time dependence of the operators $\hat{g}_{\mathbf{n}}(t)$ and $\hat{e}_{\mathbf{q}}(t)$ is specified in section 4.2 below. They satisfy the bosonic or fermionic equal-time commutation relations. In terms of these field operators, the atom-field interaction H_{AF} in eqn. (2.1) can be written as

$$H_{AF} = - \int d^3x \sum_{\alpha} \{ E_{\alpha}(x) [\mu_{\alpha}^{ge} \Psi_g^{\dagger}(x) \Psi_e(x) + \mu_{\alpha}^{eg} \Psi_e^{\dagger}(x) \Psi_g(x)] \} \quad (2.4)$$

(compare [12, eqn. (81)]). As mentioned above, it is this term that is responsible for the interaction between the surface and the atoms, as the specific form of $\mathbf{E}(\mathbf{x})$ depends on the surface. We do not make the rotating wave (or resonance) approximation here because otherwise relevant virtual processes would be missed.

We use the notation $\mathbf{r} = (\mathbf{x}, z)$ for spatial vectors, where the two-dimensional vector \mathbf{x} lies in the plane perpendicular to the surface. Spatial integrations $\int d^3r$ run only over the $z > 0$ half-space. Spacetime points are denoted by $x = (\mathbf{r}, t)$.

3 Second-order energy shift

The aim in this section is to calculate the energy shift of the atomic system due to its interaction with the electric field. In the case of a single atom in front of a surface, this shift is usually calculated in time-independent perturbation theory [9, 10, 16]. We will employ instead standard tools from field theory: the energy shift is obtained from the S -matrix, which can be perturbatively approximated with the Dyson series (see [17, sec. 3.5]). For a treatment of the single atom in front of a surface in both formalisms, nonrelativistic perturbation theory and the Dyson series, see [18, 19].

Let us briefly recall the basic relations which will be used: the energy shift of an unperturbed state of the atomic system can be calculated from the real part of the self-energy (logarithm of the S -matrix). In the present paper, we will consider only terms up to the second order in H_{AF} in which the self-energy and the T -matrix coincide. Recall that the T -matrix is defined as the nontrivial part of the S -matrix,

$$S_{fi} = \delta(f - i) - 2\pi i \delta(E_f - E_i) T_{fi}, \quad (3.1)$$

which, in turn, can be expressed as a series of time-ordered products of interaction picture operators, the Dyson series:

$$S = 1 + \sum_{n=1}^{\infty} \frac{(-i)^n}{n!} \int dt_1 \dots dt_n T \{ H_{AF}(t_1) \dots H_{AF}(t_n) \}, \quad (3.2)$$

where the symbol $T\{\dots\}$ denotes time ordering.

For a general self-interacting atomic system, it is convenient to define the interaction-picture operator

$$\Psi(x) = \Psi_g^\dagger(x)\Psi_e(x) , \quad (3.3)$$

as the operators Ψ_g and Ψ_e appear only in this combination or its hermitian conjugate in eqn. (2.4). With the initial and final states containing no excited-state atoms, the first-order term in eqn. (3.2) vanishes, leaving the second-order contribution

$$S^{(2)} = \mu_\alpha^{eg} \mu_\beta^{ge} (-i)^2 \int d^4x_1 d^4x_2 \langle \overline{\Psi(x_2)} \Psi^\dagger(x_1) \rangle D_{\alpha\beta}^F(x_2, x_1) \quad (3.4)$$

$$= \begin{array}{c} \text{---} \circ \text{---} \text{---} \circ \text{---} \\ \text{N} \quad \text{N-1} \quad \text{N} \end{array} . \quad (3.5)$$

The brackets $\langle \dots \rangle$ in eqn. (3.4) denote an expectation value in a stationary state of the atomic Hamiltonian H_A . In the above diagram, the in- and outgoing lines represent N atoms in the state $|g\rangle$ that make up the unperturbed atomic state. The virtual state (inner line) consists of an atom in the state $|e\rangle$ (dashed line) propagating in the presence of a background field (solid line) made up of the remaining $N-1$ ground state atoms (still a large number). The vertices, where an excited atom is created or destroyed, are proportional to the dipole moment of the transition:

$$\text{---} \overset{\times}{\circ} \text{---} = -i\mu_\alpha^{eg} , \quad \text{---} \underset{\times}{\circ} \text{---} = -i\mu_\alpha^{ge} . \quad (3.6)$$

The photon line in eqn. (3.5) is given by the time-ordered (or Feynman) propagator

$$D_{\alpha\beta}^F(x_1; x_2) = \text{---} \text{---} \text{---} = \langle T \{ E_\alpha(x_1) E_\beta(x_2) \} \rangle \quad (3.7)$$

$$= \int \frac{d\omega}{2\pi} e^{i\omega(t_1-t_2)} \tilde{D}_{\alpha\beta}^F(\mathbf{r}_1, \mathbf{r}_2; \omega) , \quad (3.8)$$

where the brackets $\langle \dots \rangle$ in eqn. (3.7) denote an expectation value with respect to an equilibrium state of H_F .

Finally, the contraction in eqn. (3.4) is defined as

$$\overline{\Psi(x_2)} \Psi^\dagger(x_1) = [\Psi(x_2), \Psi^\dagger(x_1)] \Theta(t_2 - t_1) . \quad (3.9)$$

which can be decomposed for bosonic or fermionic fields (upper/lower sign) as

$$\begin{aligned} \overline{\Psi(x_2)} \Psi^\dagger(x_1) &= \Theta(t_2 - t_1) \{ \pm [\Psi_g^\dagger(x_2), \Psi_e^\dagger(x_1)]_\mp [\Psi_e(x_2), \Psi_g(x_1)]_\mp \\ &\quad + \Psi_g^\dagger(x_2) [\Psi_e(x_2), \Psi_e^\dagger(x_1)]_\mp \Psi_g(x_1) \pm \Psi_e^\dagger(x_1) [\Psi_g^\dagger(x_2), \Psi_g(x_1)]_\mp \Psi_e(x_2) \\ &\quad + [\Psi_g^\dagger(x_2), \Psi_e^\dagger(x_1)]_\mp \Psi_g(x_1) \Psi_e(x_2) + \Psi_e^\dagger(x_1) \Psi_g^\dagger(x_2) [\Psi_e(x_2), \Psi_g(x_1)]_\mp \} . \end{aligned} \quad (3.10)$$

If our initial and final states contain no excited atoms, the last three terms will yield zero in an expectation value, and we are left with

$$\langle \overline{\Psi(x_2)} \Psi^\dagger(x_1) \rangle = \langle \Psi_g^\dagger(x_2) \Psi_e(x_2) \Psi_e^\dagger(x_1) \Psi_g(x_1) \rangle \Theta(t_2 - t_1) = \text{---} \text{---} \text{---} \quad (3.11)$$

for both statistics.

We will see in eqn. (4.17) below that for an ideal gas, the above expression reduces to the form that is usually obtained from applying Wick's theorem to a time-ordered product of four interaction picture operators (see [11, chap. 3]). This is no longer true in the general case (interacting atoms), and the Feynman-rules for translating a diagram containing a line like eqn. (3.11) must take into account the presence of other lines due to the interaction with the background field.

4 Photon and atom propagators

In order to evaluate the general expression eqn. (3.4), we now need to assume a concrete form for the function $D_{\alpha\beta}^F$ of eqn. (3.7) — the propagator of the electric field in the presence of a surface — and for the expression $\langle \Psi_g^\dagger(x_2) \Psi_e(x_2) \Psi_e^\dagger(x_1) \Psi_g(x_1) \rangle$ in eqn. (3.11), characterizing the atomic ensemble. For the former, we can rely largely on work presented in [10], which will allow us to apply our technique to very general surface materials. Concerning the latter, we will focus on a pure condensate in a trap (section 4.2.1) and on a trapped ideal Bose gas at nonzero temperature (section 4.2.2).

4.1 Photon propagator near a surface

The time-ordered propagator for the \mathbf{E} -field [eqn. (3.7)] is usually worked out explicitly from a mode expansion of the \mathbf{E} -field. This can be done in the presence of a non-dispersive surface, too, with the mode functions getting of course more cumbersome to satisfy the boundary conditions at the surface [19, 20]. We want to follow here the approach of [9, 10, 21], which connects the field propagator to a form involving correlation functions from linear response theory, the retarded Green functions. This applies as long as the fluctuation-dissipation theorem for the electromagnetic field holds [21, 22].

The retarded Green function for the electric field is defined as

$$G_{\alpha\beta}(x_1, x_2) = i \langle [E_\alpha(x_1), E_\beta(x_2)] \rangle \Theta(t_1 - t_2) \quad (4.1)$$

with Fourier transform $G_{\alpha\beta}(\mathbf{r}_1, \mathbf{r}_2, \omega)$. By rearranging the time ordered product in eqn. (3.7) and using the fluctuation-dissipation theorem (see [10, appendix B]) we can express the Fourier transform of the Feynman-propagator eqn. (3.8) as

$$\tilde{D}_{\alpha\beta}^F(\mathbf{r}_1, \mathbf{r}_2, \omega) = \text{Im} [G_{\alpha\beta}(\mathbf{r}_1, \mathbf{r}_2, \omega)] \coth\left[\frac{\omega}{2T}\right] - i \text{Re} [G_{\alpha\beta}(\mathbf{r}_1, \mathbf{r}_2, \omega)] \quad (4.2)$$

(see [11, sec. 31]), where T is the temperature ($k_B = 1$) of the field. Here we assume the field and its sources in thermal equilibrium at the temperature T_F . The atomic part of the system may have a different temperature and is even allowed to be in a non-thermal state. As we will see below, it is preferable to integrate the retarded Green function along the imaginary frequency axis. Using the fact that $G_{\alpha\beta}(\omega)$ has only poles in the lower half of the complex ω -plane, we can express the ω -integration in $\langle N_0 | T^{(2)} | N_0 \rangle$ (see eqn. (5.1) below) as (see [16, Appendix A]):

$$\int d\omega \frac{\tilde{D}_{\alpha\beta}^F(\omega)}{\bar{\omega}_0 - \omega - i\epsilon} \approx 2 \int_0^\infty d\xi G_{\alpha\beta}(i\xi) \frac{\bar{\omega}_0}{\bar{\omega}_0^2 + \xi^2} + 2\pi G_{\alpha\beta}(-\bar{\omega}_0) \Theta(-\bar{\omega}_0), \quad (4.3)$$

where $\bar{\omega}_0 = \omega_{eg}(\mathbf{q}, N_0)$. We have made here the approximation $\bar{\omega}_0 \gg T_F$, i.e., field temperatures much smaller than the atomic transition energies, where the summation over the poles of $\coth(\omega/2T)$ can be replaced by an integral. The second term on the rhs of eqn. (4.3) is nonzero only for excited state atoms ($\bar{\omega}_0 < 0$) and describes spontaneous emission and resonant contributions to the energy shift [16, 23]. For atoms in the ground state, corrections to Eq.(4.3) are proportional to the number of thermal photons which is exponentially small if T_F is much smaller than the relevant transition frequencies. When using eqn. (4.3) in the remaining sections, we will suppose throughout that the number of thermal photons is negligible, and any temperature dependence that appears from now on is always associated with the temperature of the atoms, not the photon field. The generalization to finite field temperatures is left for future work.

Now, from linear response theory (see [11, sec. 32]) and the linearity of the Maxwell equations, the response function $G_{\alpha\beta}(\mathbf{r}_1, \mathbf{r}_2, \omega)$ can be identified with the classical Green function, i.e., the electric field at \mathbf{r}_1 generated by a classical dipole, oscillating at frequency ω , which is located at \mathbf{r}_2 . The explicit form of the Green function in the presence of an interface is well known [24] and can be split into a free space and a reflected part:

$$G_{\alpha\beta} = G_{\alpha\beta}^0 + G_{\alpha\beta}^R \quad (4.4)$$

where $G_{\alpha\beta}^0$ is the retarded Green function in free space. As we are only interested in that part of the energy shift caused by the presence of the surface, we will not consider $G_{\alpha\beta}^0$ at all. The decomposition eqn. (4.4) permits us in a simple manner to subtract the divergent diagrams involving photon loops that yield the free-space Lamb shift, because the latter arise from the Green function $G_{\alpha\beta}^0$. To get the distance-dependent part of the energy shift, we will simply substitute $G_{\alpha\beta}$ by $G_{\alpha\beta}^R$. The expressions containing $G_{\alpha\beta}^R$ are then finite without any further renormalization.

The surface contribution $G_{\alpha\beta}^R$ at imaginary frequencies has the form

$$G_{\alpha\beta}^R(\mathbf{r}_1, \mathbf{r}_2, i\xi) = -\frac{\mu_0 \xi^2}{2\pi} \int \frac{d^2k}{\kappa} R_{\alpha\beta}(\xi, \mathbf{k}) e^{-\kappa(z_1+z_2)} e^{i\mathbf{k}\cdot(\mathbf{x}_1-\mathbf{x}_2)}, \quad (4.5)$$

(see [9,24] and below in appendix A for more details) where $\mu_0 = (\varepsilon_0 c^2)^{-1}$ is the vacuum permeability and $\kappa = \sqrt{\xi^2/c^2 + k^2}$. The two-dimensional vectors \mathbf{x} and \mathbf{k} denote position and momentum vectors parallel to the surface, respectively. The tensor elements $R_{\alpha\beta}$ contain the reflection coefficients appropriate for the specific surface material. As we are only considering the reflected part $G_{\alpha\beta}^R$, we will in the following skip the label 'R' from eqn. (4.5). Note that from the viewpoint of perturbation theory, the surface response functions $R_{\alpha\beta}$ depend on the quantum state of matter in the surface; they are calculated, of course, in the absence of the atomic system outside it.

4.2 Propagators for atoms

In the following, we calculate the atomic part of expression eqn. (3.4) for two simple examples of atomic systems. Together with the photon propagator obtained in section 4.1 above, these will finally allow us to evaluate the atom-surface interaction in section 5 and section 6.

4.2.1 Dilute interacting BEC in the single mode approximation

For the interacting dilute Bose gas confined in a trap, we further restrict ourselves to the deeply degenerate case, where we can consider a large number N_0 of atoms in a single condensate mode. We leave the contribution of condensate (Bogoliubov) excitations for future work. The atomic Hamiltonian H_A describes two-level atoms with a contact interaction between excited and ground state atoms:

$$H_A = E(g_0^\dagger g_0) + \int d^3q (\omega_{kin}^e(\mathbf{q}) + b_{ge} g_0^\dagger g_0) e_{\mathbf{q}}^\dagger e_{\mathbf{q}} \quad (4.6)$$

Here, the energy $\omega_e(\mathbf{q}) = \omega_e + \mathbf{q}^2/2M$ contains both the electronic excitation energy and the kinetic energy. The constant b_{ge} characterizes the interaction between ground- and excited state atoms. The self-interaction amongst the ground state atoms and the effects of the trapping-potential are contained in $E(g_0^\dagger g_0)$. In our approximation, the field operator Ψ_g in eqn. (2.2) consists only of a single mode with the mode function $\phi_0(\mathbf{r})$, which is the condensate wavefunction calculated self-consistently by solving the Gross-Pitaevskii-equation (GPE) [25]

$$\left[-\frac{\nabla^2}{2M} + V_{ig}(\mathbf{r}) + b_{gg}(N_0 - 1)|\phi_0(r)|^2 \right] \phi_0(\mathbf{r}) = \mu(N_0) \phi_0(\mathbf{r}). \quad (4.7)$$

Here, $\mu(N) = \partial E(N)/\partial N$ denotes the chemical potential, the constant b_{gg} characterizes the self-interaction of ground-state atoms, V_{ig} denotes the trapping potential felt by the ground-state atoms, and the condensate wavefunction is normalized to $\int d^3r |\phi_0(\mathbf{r})|^2 = 1$.

Interactions between excited state atoms are neglected in this paper. This is legitimate since our unperturbed state consists of a large number of ground state atoms. Excited state atoms will then only occur in virtual states, and their number will be small.

With the particular choice eqn. (4.6) for H_A , the field operators Ψ_g and Ψ_e from eqn. (2.2) and eqn. (2.3) assume the form

$$\Psi_g(x) = \phi_0(\mathbf{r}) \exp[-i(E_g(\hat{N}_0 + 1) - E_g(\hat{N}_0) + b_{ge}\hat{N}_e)t] \hat{g}_0, \quad (4.8)$$

$$\Psi_e(x) = \int \frac{d^3q}{(2\pi)^{3/2}} \exp[i(\mathbf{q}\cdot\mathbf{r} - (\omega_{kin}^e(\mathbf{q}) + b_{ge}\hat{N}_0)t)] \hat{e}_{\mathbf{q}}. \quad (4.9)$$

The diagram eqn. (3.11) then becomes

$$\begin{array}{c} \xrightarrow{N_0} \text{---} \xrightarrow{N_0} \\ \text{---} \end{array} = \Theta(t_2 - t_1) \phi_0(\mathbf{r}_1) \phi_0^*(\mathbf{r}_2) N_0 \int \frac{d^3q}{(2\pi)^3} e^{i\mathbf{q}\cdot(\mathbf{r}_2 - \mathbf{r}_1)} \times e^{-i\omega_{eg}(\mathbf{q}, N_0)(t_2 - t_1)}. \quad (4.10)$$

Here the transition frequency $\omega_{eg}(\mathbf{q}, N)$ is defined as

$$\omega_{eg}(\mathbf{q}, N) = \omega_e(\mathbf{q}) + E_g(N - 1) - E_g(N) + (N - 1)b_{ge}, \quad (4.11)$$

where the frequency shift of the atomic transition due to inter-atomic interactions appears. If the system consists of a single atom only,

$$\omega_{eg}(\mathbf{q}, 1) = \omega_e(\mathbf{q}) - \omega_g = \omega_{eg} + \frac{\mathbf{q}^2}{2M}, \quad (4.12)$$

which is the resonance frequency of a single atom, including the recoil shift. The physical interpretation of Eq.(4.10) is quite clear: a virtual photon takes a ground state atom at position \mathbf{r}_1 to the excited state, the atom propagates freely to position \mathbf{r}_2 and joins the other ground state atoms there. We shall see below that the relevant distances $|\mathbf{r}_2 - \mathbf{r}_1|$ are negligibly small so that eventually the ground-state density $|\phi_0(\mathbf{r}_1)|^2$ determines the atom-surface interaction.

4.2.2 Ideal Bose gas at finite temperature

For the non-interacting trapped Bose gas, treated in the grand-canonical ensemble with a mean total particle number N , an inverse temperature β and chemical potential μ , the Hamiltonian H_A takes the form

$$H_A = \sum_{\mathbf{n}} E_{\mathbf{n}} + \int d^3q \omega_{kin}^e(\mathbf{q}) \hat{e}_{\mathbf{q}}^\dagger \hat{e}_{\mathbf{q}}. \quad (4.13)$$

The mode functions for the operator Ψ_g are the single-particle wavefunctions $\phi_{\mathbf{n}}$ that solve

$$\left[-\frac{\nabla^2}{2M} + V_{tg}(\mathbf{r})\right] \phi_{\mathbf{n}}(\mathbf{x}) = E_{\mathbf{n}} \phi_{\mathbf{n}}(\mathbf{x}). \quad (4.14)$$

The field operators eqn. (2.2) and eqn. (2.3) now take the simple form

$$\Psi_g(x) = \sum_{\mathbf{n}} \phi_{\mathbf{n}}(\mathbf{r}) e^{-iE_{\mathbf{n}}t} \hat{g}_{\mathbf{n}}, \quad (4.15)$$

$$\Psi_e(x) = \int \frac{d^3q}{(2\pi)^{3/2}} e^{i(\mathbf{q}\cdot\mathbf{r} - \omega_{kin}^e(\mathbf{q})t)} \hat{e}_{\mathbf{q}}. \quad (4.16)$$

The atomic part eqn. (3.11) yields

$$\begin{array}{c} \xrightarrow{N, \mu, \beta} \text{---} \xrightarrow{N, \mu, \beta} \\ \text{---} \end{array} = \langle \Psi_g^\dagger(x_2) \Psi_g(x_1) \rangle \overline{\Psi_e(x_2) \Psi_e^\dagger(x_1)} \quad (4.17)$$

$$\begin{aligned} &= \Theta(t_2 - t_1) \sum_{\mathbf{n}} \phi_{\mathbf{n}}^*(\mathbf{r}_2) \phi_{\mathbf{n}}(\mathbf{r}_1) e^{iE_{\mathbf{n}}(t_2 - t_1)} \langle \hat{g}_{\mathbf{n}}^\dagger \hat{g}_{\mathbf{n}} \rangle \\ &\times \int \frac{d^3q}{(2\pi)^3} \exp[i\mathbf{q}\cdot(\mathbf{r}_2 - \mathbf{r}_1) - i(q^2/(2m) + \omega_{eg})(t_2 - t_1)] \end{aligned} \quad (4.18)$$

Note again the occurrence of the two-point correlation function for the ground-state atoms. We thus reach a similar structure as in Eq.(4.10) above, but with a sum over all trap eigenstates.

5 Energy shift of an interacting Bose gas trapped near a surface

5.1 Generalized polarizability

With the results obtained above, we can now evaluate the interaction potential between the single-mode condensate and a surface. Putting the expression for the photon propagator eqn. (3.7) and for the atomic two-point function eqn. (4.10) into eqn. (3.4), we get for the T -matrix element (after performing the dt_1 and dt_2 integrations)

$$\begin{aligned} \langle N_0 | T^{(2)} | N_0 \rangle &= N_0 \mu_\alpha^{ge} \mu_\beta^{eg} \int d^3 r_1 \int d^3 r_2 \phi_0(\mathbf{r}_2) \phi_0^*(\mathbf{r}_1) \\ &\times \int \frac{d\omega}{2\pi} \tilde{D}_{\alpha\beta}^F(\mathbf{r}_1, \mathbf{r}_2, \omega) \int \frac{d^3 q}{(2\pi)^3} \frac{e^{i\mathbf{q}\cdot(\mathbf{r}_1 - \mathbf{r}_2)}}{\omega - \omega_{eg}(\mathbf{q}, N_0) + i\epsilon}, \end{aligned} \quad (5.1)$$

Using relation eqn. (4.3) in eqn. (5.1) to link the time-ordered photon propagator to the Green tensor $G_{\alpha\beta}$, we get

$$\begin{aligned} \langle N_0 | T^{(2)} | N_0 \rangle &= -N_0 \frac{2}{(2\pi)^4} \mu_\alpha^{ge} \mu_\beta^{eg} \int d^3 r_1 \int d^3 r_2 \phi_0(\mathbf{r}_2) \phi_0^*(\mathbf{r}_1) \\ &\times \int_0^\infty d\xi G_{\alpha\beta}(\mathbf{r}_1, \mathbf{r}_2, i\xi) \int d^3 q a(\mathbf{q}, \xi) e^{i\mathbf{q}\cdot(\mathbf{r}_1 - \mathbf{r}_2)}, \end{aligned} \quad (5.2)$$

The generalized polarizability

$$a(\mathbf{q}, \xi) = \frac{\omega_{eg}(\mathbf{q}, N_0)}{\omega_{eg}^2(\mathbf{q}, N_0) + \xi^2}. \quad (5.3)$$

contains the interaction- and recoil-shifted resonance frequency $\omega_{eg}(\mathbf{q}, N_0)$ (see eqn. (4.11)). In eqn. (5.2) we neglected the resonant contribution of thermally excited photons.

5.2 Condensate wave function

In order to evaluate eqn. (5.2), we have to substitute a suitable approximation for the condensate wave function $\phi_0(\mathbf{r})$. For simplicity we solve the Gross-Pitaevskii equation eqn. (4.7) with an isotropic harmonic trapping potential

$$V_{tg}(\mathbf{r}) = \frac{M}{2} \nu^2 (\mathbf{x}^2 + (z - d)^2), \quad (5.4)$$

where d denotes the distance of the trap center from the surface. If the kinetic term in the GPE can be neglected (Thomas-Fermi approximation), the solution for the density profile takes the form of an inverted parabola. This is usually a good approximation for large particle numbers. Here, we choose a Gaussian ansatz for the wave function because it simplifies the subsequent integrations. (For calculations with a Thomas-Fermi profile, see [26].) The ansatz also allows for the limit $N_0 \rightarrow 1$ in order to provide a cross-check with results for a single-atom system (section 5.4). Gaussian functions also approximately solve the GPE, if width and amplitude are varied such that the Gross-Pitaevskii functional is minimized (see [25] for details). We thus make the ansatz

$$\phi_0(\mathbf{r}) = (\sqrt{\pi} \sigma(N_0))^{-\frac{3}{2}} \exp \left[-\frac{\mathbf{x}^2 + (z - d)^2}{2\sigma^2(N_0)} \right]. \quad (5.5)$$

The minimization procedure gives a spatial width $\sigma(N_0)$ in eqn. (5.5) that depends on the number of trapped particles and has the asymptotic values [27]

$$\sigma(N_0) = \begin{cases} a_0, & N_0 = 1 \\ a_0 \left(\sqrt{\frac{2}{\pi}} \frac{N_0 a}{a_0} \right)^{1/5}, & \frac{N_0 a}{a_0} \gg 1 \end{cases}. \quad (5.6)$$

where $a_0 = (M\nu)^{-1/2}$ is the width of the single-particle ground state in the trap. The s -wave scattering length a is related to the interaction constant b_{gg} from eqn. (4.7) via $b_{gg} = 4\pi a/M$. In the second case of eqn. (5.6), the interaction energy of ground state atoms is much larger than the bare harmonic potential. This regime corresponds to the Thomas-Fermi limit (the Thomas-Fermi radius is $R_{\text{TF}} = a_0(15N_0a/a_0)^{1/5}$).

A subtlety arises for the Gaussian ansatz (5.5) because it is normalized only in the limit $d \gg \sigma(N_0)$ if spatial integrations are restricted over the half-space $z > 0$. We shall always assume this limit, as our approach is clearly not valid for atoms touching the surface. The wave function ϕ_0 is of the order $\mathcal{O}(\exp[-(d/\sigma(N_0))^2])$ at the surface, and exponentially small terms of this order will be systematically discarded in numerical evaluations of energy shifts in section 5.4 and section 6. These approximations are dealt with in detail in appendix B.

In the following, we will evaluate $T_{N_0N_0}^{(2)}$ with the approximate ground-state wave function ϕ_0 from eqn. (5.5). The result eqn. (5.2) for the T -matrix is, however, more generally valid and can be evaluated similarly for other approximations of $\phi_0(\mathbf{r})$.

5.3 Recoil shift and (de)localization correction

At this stage, it is convenient to introduce sum and difference coordinates \mathbf{r}_\pm and to split them in components perpendicular and parallel to the surface: $z_\pm = z_1 \pm z_2$, and $\mathbf{x}_\pm = \mathbf{x}_1 \pm \mathbf{x}_2$. Similarly, for the momentum, we use from now on $\mathbf{q} = (q_x, q_y, q_z) \rightarrow (\mathbf{q}, q_z)$. Integrating in eqn. (5.2) over \mathbf{r}_1 and \mathbf{r}_2 and the angle of the two-dimensional vectors \mathbf{k} and \mathbf{q} ($\mathbf{k} \cdot \mathbf{k} = k^2$ and $\mathbf{q} \cdot \mathbf{q} = q^2$), we get

$$\begin{aligned} \langle N_0 | T^{(2)} | N_0 \rangle &= -N_0 \frac{2\sigma^3}{\pi^{3/2}} \frac{\mu_\alpha^{ge} \mu_\beta^{eg}}{\varepsilon_0} \int_0^\infty d\xi \int_0^\infty \frac{k dk}{\kappa} \frac{1}{2} e^{-2\kappa d} e^{\kappa^2 \sigma^2} (1 + \text{erf}[\frac{d}{\sigma} - \kappa\sigma]) M_{\alpha\beta} \\ &\times \int_0^\infty dq_z \int_0^\infty q dq a(q, q_z, \xi) I_0[2\sigma^2 kq] e^{-(k^2 + q^2 + q_z^2)\sigma^2}, \end{aligned} \quad (5.7)$$

with an obvious notation for $a(q, q_z, \xi)$. The diagonal matrix $M_{\alpha\beta}$ originates from the scattering tensor $R_{\alpha\beta}$ and has elements

$$M_{xx}(k, \xi) = M_{yy}(k, \xi) = R^p k^2 + (R^p - R^s) (\xi/c)^2, \quad (5.8)$$

$$M_{zz}(k, \xi) = 2R^p k^2, \quad (5.9)$$

and the $R^{s,p}(k, \xi)$ are the reflection amplitudes from the surface (eqns. (A.3) and (A.4)), I_0 is a Bessel function of the second kind, $\kappa = \sqrt{k^2 + \xi^2}$, and erf denotes the error function.

To perform the dq_z and dq -integrations in eqn. (5.7), we observe that in $a(q, q_z, \xi)$ (see eqn. (5.3)) the momenta q and q_z appear only as recoil shifts of the atomic transition frequency $\omega_{eg}(N_0)$ (see eqn. (4.11)). Since the relevant momenta are limited to typically $1/\sigma$, the recoil shift is a small correction because $1/(M\sigma^2) = \nu \ll \omega_{eg}(N_0)$ is usually well satisfied. We therefore expand in powers of q and q_z and integrate term by term by means of the identities

$$\int_0^\infty q dq e^{-(k^2 + q^2)\sigma^2} I_0[2kq\sigma^2] = \frac{1}{2\sigma^2}, \quad (5.10)$$

$$\int_0^\infty q dq q^2 e^{-(k^2 + q^2)\sigma^2} I_0[2kq\sigma^2] = \frac{1}{2\sigma^2} \left(\frac{1}{\sigma^2} + k^2 \right). \quad (5.11)$$

Thus, we finally obtain for the T -matrix eqn. (5.7)

$$\begin{aligned} \langle N_0 | T^{(2)} | N_0 \rangle &= -\frac{N_0}{2\pi} \frac{\mu_\alpha^{ge} \mu_\beta^{eg}}{\varepsilon_0} \int_0^\infty d\xi \int_0^\infty \frac{k dk}{\kappa} \frac{1}{2} e^{-2\kappa d} e^{\kappa^2 \sigma^2} (1 + \text{erf}[\frac{d}{\sigma} - \kappa\sigma]) M_{\alpha\beta} \\ &\times \{ \alpha(\xi, N_0) + \alpha^{(rc)}(\xi, N_0, k) \} \end{aligned} \quad (5.12)$$

where the polarizability

$$\alpha(\xi, N_0) = \frac{\omega_{eg}(N_0)}{\omega_{eg}(N_0)^2 + \xi^2}, \quad (5.13)$$

describes the no-recoil case. The recoil term $\alpha^{(rc)}$ is given by

$$\alpha^{(rc)}(\xi, N_0, k) = -\frac{\omega_{eg}(N_0)^2 - \xi^2}{(\omega_{eg}(N_0)^2 + \xi^2)^2} \left(\frac{3}{4M(\sigma(N_0))^2} + \frac{k^2}{2M} \right). \quad (5.14)$$

We can attribute this correction to a recoil shift of the effective resonance frequency

$$\omega_{eg} \rightarrow \omega_{eg} + \frac{3}{4M(\sigma(N_0))^2} + \frac{k^2}{2M} \quad (5.15)$$

where the two terms describe the kinetic energy from the delocalized condensate wave function and from the absorbed photon momentum in the excited state, respectively.

The T-matrix element $T_{N_0 N_0}^{(2)}$ from eqn. (5.12) is our main result for the interaction energy of a trapped Bose gas with a plane surface. In the above form, it is clear that $T_{N_0 N_0}^{(2)}$ generalizes the result for a stationary single atom in a straightforward manner. Clearly, as we put $N_0 = 1$, we get the single-atom transition frequency $\omega_{eg}(1) = \omega_{eg}$. And with the identity

$$\lim_{\sigma \rightarrow 0} \frac{1}{2} e^{-2\kappa d} e^{\kappa^2 \sigma^2} (1 + \operatorname{erf}[\frac{d}{\sigma} - \kappa\sigma]) = e^{-2\kappa d}, \quad (5.16)$$

we get from the no-recoil term of eqn. (5.12)

$$\lim_{\sigma \rightarrow 0} T_{11}^{(2)} = -\frac{1}{\pi} \mu_\alpha^{ge} \mu_\beta^{eg} \int_0^\infty d\xi G_{\alpha\beta}^R(\mathbf{r}_0, \mathbf{r}_0, i\xi) \frac{\omega_{eg}}{\omega_{eg}^2 + \xi^2} \quad (5.17)$$

with $\mathbf{r}_0 = (0, 0, d)$ the position of the trap center. This is the known result for a perfectly localized single atom as in Ref. [10, eqn. (2.28)]. The recoil correction involving $\alpha^{(rc)}$ is discussed in more detail in section 5.4. It is usually very small, unless the trap frequency ν is comparable to the atomic resonance ω_{eg} , a case of no practical significance.

For a large atom number N_0 , the resonance frequency $\omega_{eg}(N_0)$ in eqn. (5.13) incorporates the interatomic interactions (see eqn. (4.11)). The overall proportionality factor N_0 of eqn. (5.12) can be understood by recalling that the responsible diagram (see eqn. (3.5)) represents a sum of self-energies of N_0 individual ground state atoms. In higher orders, i.e., diagrams with four or more vertexes, virtual photons can connect different ground state atoms, and we can expect a nonlinear scaling in N_0 .

5.4 Single ground-state atom

The T-matrix element for a single atom can be obtained from eqn. (5.12) by setting $N_0 = 1$. Introducing the scaled distance $x = d\omega_{eg}/c$, and rescaling the integration variables $\bar{\xi} = \xi/\omega_{eg}$, $\bar{k} = ck/\omega_{eg}$, $\bar{\kappa} = c\kappa/\omega_{eg}$, the T-matrix reads

$$\begin{aligned} \langle 1|T^{(2)}|1\rangle &= -\frac{\mu_\alpha^{ge} \mu_\beta^{eg} \omega_{eg}^3}{2\pi\epsilon_0 c^3} \int_0^\infty d\bar{\xi} \int_0^\infty \frac{\bar{k} d\bar{k}}{\bar{\kappa}} I(\bar{\kappa}, x, \eta) M_{\alpha\beta}(\bar{k}, \bar{\xi}) \\ &\quad \times \omega_{eg} \{ \alpha(\bar{\xi}\omega_{eg}, 1) + \alpha^{(rc)}(\bar{\xi}\omega_{eg}, 1, \bar{k}\omega_{eg}) \}, \end{aligned} \quad (5.18)$$

where the energy scale is set by the natural linewidth $\gamma_{eg} = |\mu^{ge}|^2 \omega_{eg}^3 / 3\pi\epsilon_0 c^3$, the so-called Lamb-Dicke parameter $\eta = \omega_{eg} a_0 / c$ gives the size of the trap ground state in units of the resonant wavelength. The quantity I becomes

$$I(\kappa, x, \eta) \equiv \frac{1}{2} \exp[-2\bar{\kappa}x + \bar{\kappa}^2 \eta^2] (1 + \operatorname{erf}[\frac{x}{\eta} - \bar{\kappa}\eta]) \quad (5.19)$$

The matrix $M_{\alpha\beta}$ defined in eqn. (5.9) depends on the reflection coefficients R^p and R^s and encodes the surface properties. In the dimensionless units of eqn. (5.18), the recoil correction $\alpha^{(rc)}$ is now seen to be proportional to the ratio ν/ω_{eg} :

$$\omega_{eg} \alpha(\bar{\xi}\omega_{eg}, 1) = (1 + \bar{\xi}^2)^{-1}, \quad (5.20)$$

$$\omega_{eg} \alpha^{(rc)}(\bar{\xi}\omega_{eg}, 1, \bar{k}\omega_{eg}) = -\frac{\nu}{\omega_{eg}} \frac{1 - \bar{\xi}^2}{(1 + \bar{\xi}^2)^2} \left(\frac{3}{4} + \frac{\bar{k}^2}{2} \eta^2 \right) \quad (5.21)$$

The trapping frequency $\nu/2\pi$ for a single ground state atom in the potential eqn. (5.4) is usually around 10...1000 Hz, much smaller than the frequencies of optical transitions $\omega_{eg}/2\pi \approx 10^{15}$ Hz. This justifies the expansion of the recoil shift for small atom momenta \mathbf{q} done in section 5. Experimental situations where the recoil correction is enhanced in magnitude could involve tight traps like optical lattices ($\nu/2\pi \sim 100$ kHz) and Rydberg atoms whose transition frequencies can be a factor 10^6 smaller [28].

The expression in eqn. (5.18) is easily evaluated numerically. To properly eliminate the exponentially small but nonvanishing overlap of $\phi_0(\mathbf{r})$ with the surface, we cut off the k and ξ integrations at suitably large values, as explained in detail in appendix B. This procedure applies in exactly the same fashion to the integration in eqn. (6.9) below.

Figure 1 shows the energy shift of a rubidium atom in the harmonic trapping potential eqn. (5.4) with $\nu/2\pi = 1$ kHz. At this frequency, the oscillator length is $a_0 \approx 340$ nm. As the overlap of the atom wavefunction with the surface should be negligible, we restrict the evaluation to a distance range $d \geq 2 \mu m$, making an error of the order $\text{Exp}[-(d/a_0)^2] \sim 10^{-16}$. The black lines in fig. 1 are for the case of a perfectly reflecting surface, with the reflection amplitudes $R^p = 1$ and $R^s = -1$. The red lines involve a frequency-dependent reflection, as appropriate for a gold surface (described by the Drude model, see appendix A for details). The two terms of eqn. (5.18) are shown separately, the recoil correction (dashed lines) is multiplied by a factor of $-\omega_{eg}/\nu$ to fit on the scale. The dashed horizontal line shows the asymptotic expression for the Casimir-Polder potential of an atom in front of a perfect mirror,

$$\Delta E_{CP}(d) = -\frac{c\alpha(0)}{\epsilon_0 d^4} \frac{3}{8\pi}, \quad (5.22)$$

with the static polarizability $\alpha(0)$.

6 Ideal Bose gas in a surface trap

Now we will use the results obtained in section 4.2.2 to calculate the atom-surface interaction for a gas of N noninteracting bosons. The atomic system (treated in the grand-canonical ensemble) is supposed to be in thermal equilibrium at the inverse temperature β , but its temperature is allowed to be different from the field temperature.

6.1 Atomic correlation function

As above in section 5, we will assume an isotropic harmonic trapping potential of the form eqn. (5.4). For the ideal Bose gas, $\phi_{\mathbf{n}}$ and $E_{\mathbf{n}}$ that enter the expression eqn. (4.15) for Ψ_g are then simply the eigenfunctions and energies of a three-dimensional harmonic oscillator:

$$E_{\mathbf{n}} = (n_x + n_y + n_z)\nu, \quad n_i = 0, 1, 2, \dots, \quad (6.1)$$

where the ground state of the trap has been set equal to the zero of energy. The critical temperature takes the value [25, 29]

$$T_c = \nu \left(\frac{N}{\zeta[3]} \right)^{1/3}. \quad (6.2)$$

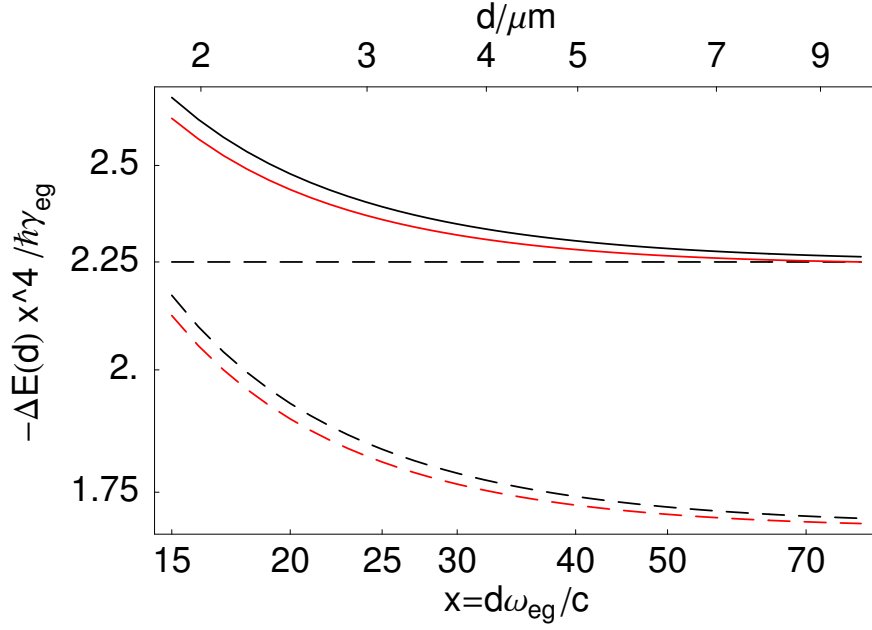


Figure 1: Atom-surface interaction energy between a rubidium atom and a perfectly reflecting (black/upper solid) and gold surface (red/lower solid), field at zero temperature. Distance $d = xc/\omega_{eg}$ in units of the resonance wavelength, energy multiplied by x^4 and scaled by the natural linewidth $\hbar\gamma_{eg} = |\boldsymbol{\mu}^{eg}|^2\omega_{eg}^3/(3\pi\epsilon_0c^3)$. The atom is trapped in the harmonic potential eqn. (5.4) with a trap frequency $\nu/2\pi = 1$ kHz. Dashed lines: recoil correction multiplied by $-\omega_{eg}/\nu$ (see eqn. (5.18)). Resonance frequency $\omega_{eg} = 2\pi 3.85 \times 10^{14}$ Hz (isotropic polarizability); parameters of the Drude dielectric function for gold, eqn. (A.5): $\omega_p = 5.74\omega_{eg}$ and $\omega_p\tau = 5 \times 10^3$.

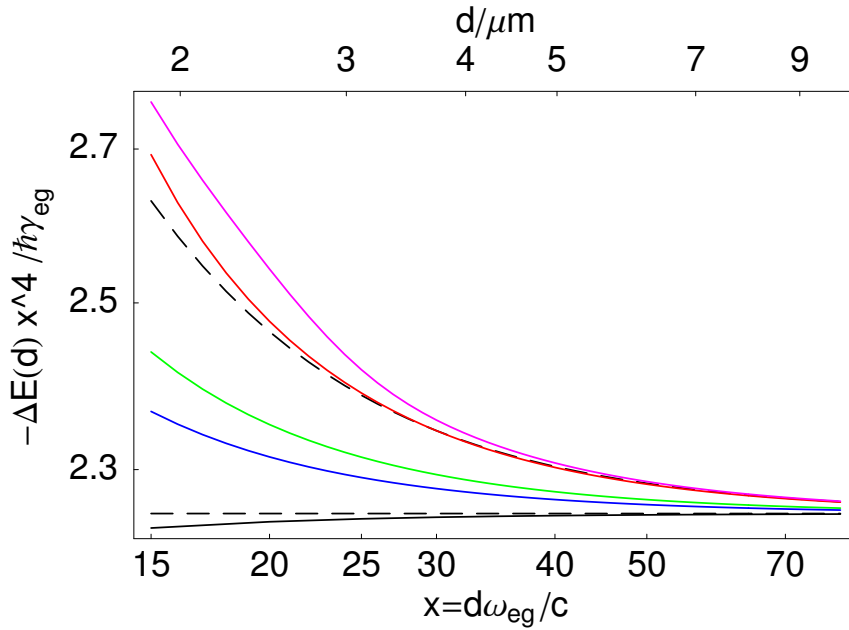


Figure 2: Atom-surface interaction between a trapped rubidium atom and a perfectly reflecting surface (field at zero temperature). Energy scaled by d^4 as in fig. 1. The full curves correspond to a perfectly localized atom (black/bottom) and delocalized atoms with different trapping frequencies ($\nu/2\pi = 3, 2, 1$ kHz in blue, green, red from bottom to top). Top/pink curve: interaction energy per atom for a trapped ideal Bose gas at $T = 0.2T_c$ and $\nu/2\pi = 1$ kHz (see eqn. (6.9)). Horizontal dashed line: asymptotic expression ΔE_{CP} (see eqn. (5.22)) for the Casimir-Polder potential. Dashed curve: ΔE_{CP} multiplied with the enhancement factor eqn. (6.12) for $\nu/2\pi = 1$ kHz.

For a given mean particle number N and inverse temperature β , the (negative valued) chemical potential $\mu(N, \beta)$ has to be determined from the relation

$$N(\mu, \beta) = \int d^3r \langle \Psi_g^\dagger(\mathbf{r}) \Psi_g(\mathbf{r}) \rangle, \quad (6.3)$$

where the brackets $\langle \dots \rangle$ denote a state of the atomic system at temperature β .

With the same arguments as in section 5.3 above, the propagator for the excited atomic state is local to a very good approximation. Neglecting the small recoil correction, we find from eqn. (4.18)

$$\begin{aligned} \langle \Psi_g^\dagger(x_2) \Psi_g(x_1) \rangle \overline{\Psi_e(x_2) \Psi_e^\dagger(x_1)} &\approx \sum_{\mathbf{n}} \frac{\Phi_{\mathbf{n}}^*(\mathbf{r}_2) \Phi_{\mathbf{n}}(\mathbf{r}_1)}{\exp[\beta(E_{\mathbf{n}} - \mu)] - 1} \exp[-i(t_2 - t_1)(\omega_{eg} - E_{\mathbf{n}})] \\ &\times \Theta(t_2 - t_1) \delta(\mathbf{r}_2 - \mathbf{r}_1). \end{aligned} \quad (6.4)$$

To the same precision, we can neglect the single particle energy $E_{\mathbf{n}}$ compared to the atomic transition energy ω_{eg} . This is even true for realistic atom temperatures: for a trapping frequency $\nu/2\pi = 1$ kHz and a mean number of $N = 10^4$ trapped particles, the mean thermal energy that sets the scale for the relevant $E_{\mathbf{n}}$ evaluates to $T = (T/T_c) 2\pi \cdot 20.3$ kHz much smaller than ω_{eg} . We thus neglect $E_{\mathbf{n}}$ in the exponential in eqn. (6.4) and obtain

$$\overline{\Psi_g^\dagger(x_2) \Psi_g(x_1)} \approx \Theta(t_2 - t_1) \delta(\mathbf{r}_2 - \mathbf{r}_1) \langle \Psi_g^\dagger(\mathbf{r}_2) \Psi_g(\mathbf{r}_1) \rangle e^{-i\omega_{eg}(t_2 - t_1)}. \quad (6.5)$$

The correlation function $\langle \Psi_g^\dagger(\mathbf{r}_2) \Psi_g(\mathbf{r}_1) \rangle$ that enters in eqn. (6.3) and in eqn. (6.5) above reads [25, 29]

$$\begin{aligned} \langle \Psi_g^\dagger(x_2) \Psi_g(x_1) \rangle &= (\sqrt{\pi}a_0)^{-3} \sum_{j=1}^{\infty} \left\{ e^{j\beta\mu} (1 - e^{-2j\beta\nu})^{-3/2} \right. \\ &\times \exp \left[-\frac{1}{4a_0^2} (|\mathbf{r}_2^d + \mathbf{r}_1^d|^2 \tanh[j\beta\nu/2] + |\mathbf{r}_2^d - \mathbf{r}_1^d|^2 \coth[j\beta\nu/2]) \right] \left. \right\} \end{aligned} \quad (6.6)$$

where the vectors $\mathbf{r}^d \equiv (\mathbf{x}, z - d)$ account for the distance d between the surface and the center of the trap.

6.2 Surface-induced energy shift

With these approximations, the general expression eqn. (3.4) gives a T -matrix

$$\langle N|T^{(2)}|N \rangle = \mu_\alpha \mu_\beta \int d^3r \langle \Psi_g^\dagger(\mathbf{r}) \Psi_g(\mathbf{r}) \rangle \int \frac{d\omega}{2\pi} \frac{\tilde{D}_{\alpha\beta}^F(\mathbf{r}, \mathbf{r}, \omega)}{\omega - \omega_{eg} + i\epsilon}. \quad (6.7)$$

Had we kept the trap eigenenergy $E_{\mathbf{n}}$, it would appear as a small shift of ω_{eg} in the denominator. Using eqn. (4.3) and neglecting any thermal photons (see the remark below eqn. (4.3)), we obtain

$$\langle N|T^{(2)}|N \rangle = -\mu_\alpha \mu_\beta \frac{1}{\pi} \int d^3r \langle \Psi_g^\dagger(\mathbf{r}) \Psi_g(\mathbf{r}) \rangle \int_0^\infty d\xi \tilde{G}(\mathbf{r}, \mathbf{r}, i\xi) \frac{\omega_{eg}}{\omega_{eg}^2 + \xi^2}. \quad (6.8)$$

Performing the spatial integration and switching to the dimensionless variables of eqn. (5.18) yields

$$\begin{aligned} \langle N|T^{(2)}|N \rangle &= -\frac{1}{2\pi} \frac{\mu_\alpha^{ge} \mu_\beta^{eg} \omega_{eg}^3}{\varepsilon_0 c^3} \sum_{j=1}^{\infty} e^{j\beta\mu} ((1 - e^{-2j\beta\nu}) \tanh[j\beta\nu/2])^{-3/2} \\ &\times \int_0^\infty d\bar{\xi} \int_0^\infty \frac{\bar{k} d\bar{k}}{\bar{k}} I(\bar{\kappa}, x, \eta_+) M_{\alpha\beta}(\bar{k}, \bar{\xi}, R^p, R^s) \frac{1}{1 + \bar{\xi}^2}, \end{aligned} \quad (6.9)$$

where $I(\bar{\kappa}, x, \eta_+)$ is defined in eqn. (5.19), and the matrix $M_{\alpha\beta}$ in eqn. (5.9). The Lamb-Dicke parameter $\eta_+ = a_+ \omega_{eg}/c$ now involves the temperature dependent width

$$a_+ = a_0 (\tanh[j\beta\nu/2])^{-1/2} \geq a_0. \quad (6.10)$$

To compare eqn. (6.9) with the result eqn. (5.18) for the single atom, we note that the constraint eqn. (6.3) leads to

$$\sum_{j=1}^{\infty} e^{j\beta\mu} \left((1 - e^{-2j\beta\nu}) \tanh[j\beta\nu/2] \right)^{-3/2} = N \quad (6.11)$$

and consider an interaction energy per atom, $\langle N|T^{(2)}|N\rangle/N$. The terms with large j in the sum involve a width a_+ equal to the zero-temperature value a_0 . These terms describe the condensate atoms in the trap ground state. The terms with small j have larger values of a_+ and contribute to the energy shift as a broader trap would do. Indeed, for $j = 1$ and $\beta\nu \ll 1$, one gets the spatial width of a classical, thermal density distribution.

This behaviour is shown in the numerical evaluation of eqn. (6.9) and eqn. (5.18) in fig. 2, for a perfectly reflecting surface. (More realistic materials can be described without further complications.) The atom-surface interaction per atom at $T = 0.2T_c$ is larger than for a single atom (at the same trap frequency $\nu/2\pi = 1$ kHz), which is due to the larger spatial size of the thermally excited trap levels.

At an atom-surface distance of $d > 2\mu m$, the interaction potential for the perfectly localized atom (calculated from eqn. (5.17)) is already deep in the retarded x^{-4} regime. For an atom delocalized in the trap, the interaction potential becomes larger in magnitude because of the curvature of the Casimir-Polder interaction. Averaging a power law $1/z^4$ over a narrow distribution ($\sigma \ll d$) centered at $z = d$, we get to leading order the enhancement factor

$$\left\langle \frac{1}{z^4} \right\rangle \approx \frac{1}{d^4} [1 + 5(\sigma/d)^2 + \dots] . \quad (6.12)$$

The dashed black curve in fig. 2 shows the asymptotic expression for the Casimir-Polder potential eqn. (5.22) multiplied with the above enhancement factor for a trapping frequency of $\nu/2\pi = 1$ kHz. The estimate eqn. (6.12) is seen to be in good agreement with our result from eqn. (5.18) (red line).

7 Summary and outlook

The starting point of our calculation was a second-quantized Hamiltonian that describes the interaction of a trapped system of N atoms with the electromagnetic field. We have focused on two simple models for the atomic system: an interacting BEC described by N_0 atoms populating a single condensate wave function (described by the state $|N_0\rangle$) and a noninteracting Bose gas at finite temperature, where the N particles populate the various single particle states of the trap (this state is denoted schematically by $|N\rangle$). To calculate the interaction energy between the atoms and a plane surface, we made a perturbative expansion of the electromagnetic self-energy and worked out the T -matrix elements $\langle N_0|T^{(2)}|N_0\rangle$ and $\langle N|T^{(2)}|N\rangle$ to second order in the atom-field coupling. The methods developed here are general enough to push the diagrammatic expansion to higher orders. The electric field propagator has been expressed in terms of retarded Green functions that permit to identify easily the contribution brought about by the surface. The characteristics of the surface material then enter through the scattering amplitudes for light, which allows for treating a wide range of materials. For the sake of simplicity, we considered the field to be at zero temperature as well, but thermal corrections can be included in a straightforward way by considering the temperature dependent term in eqn. (4.3). Even non-equilibrium situations (bodies at different temperatures) can be covered by combining the techniques of fluctuation electrodynamics [30] with the Keldysh formalism (see Ref. [31] for an example).

The expression found for $\langle N_0|T^{(2)}|N_0\rangle$ in eqn. (5.2) describes the Casimir-Polder like interaction energy of a trapped Bose gas with the surface, for a general condensate wave function $\phi_0(\mathbf{x})$. If the system is reduced to a perfectly localized single atom as treated in [10], our expression reproduces known results (see eqn. (5.17)). It also highlights that in full generality, the atom-surface interaction does not reduce to an integral over the density distribution of the atoms, due to the (virtual) propagation in the excited state. The

Bose gas-surface interaction energy shows an overall scaling with the atom number N_0 (as can be expected at this order of perturbation theory), but even the interaction energy per atom still depends weakly on N_0 . We have identified for this dependence the following physical mechanisms. (i) The interaction energy involves a spatial average over the density profile whose width is larger for repulsive atom-atom interaction. This effect was already taken into account in the pioneering experiments of Ref. [5, 7]. (ii) The atomic interactions (treated here as a contact potential) shift the optical transition frequency (see for example the experiments of Ref. [32]) and modifies the ground-state polarizability eqn. (5.13). (iii) The optical spectral line is recoil-broadened due to the kinetic energy of the atoms. This effect is very weak for typical traps and in the fully degenerate limit as the phase gradient of the condensate wave function vanishes.

For the ideal Bose gas from $\langle N|T^{(2)}|N\rangle$ in eqn. (6.9), the Casimir-Polder interaction per particle does not depend on the atom number. We showed that the influence of a higher atom temperature on the atom-surface interaction is similar to that of a broadening of the trap potential.

We plan to generalize the method presented in the present paper in two directions: on the BEC side of the problem, we want to include contributions from higher collective modes (condensate depletion, phase fluctuations, thermal density fraction) and revisit the problem of two atoms in front of a surface [33]. This setting has also been realized in a many-body version, by splitting a BEC in two spatially separated modes [34,35]. On the cavity QED side, higher orders of atom-photon interactions will be considered where intensity fluctuations of the quantum field near the surface appear [36,37].

A Retarded Green function for the electric field in the presence of an interface

The reflected part of the retarded Green function in the presence of an interface (as presented in [9, eqn. (3.4)], see also [38, sec. 2] for an overview) reads

$$G_{\alpha\beta}^{RR}(\mathbf{r}_1, \mathbf{r}_2, \omega) = -\frac{i\omega^2}{2\pi\epsilon_0 c^2} \int \frac{d^2k}{k_z} R_{\alpha\beta}(\mathbf{k}, \omega) e^{ik_z(z_1+z_2)+i\mathbf{k}\cdot(\mathbf{x}_1-\mathbf{x}_2)}, \quad (\text{A.1})$$

with $k_z = \sqrt{\omega^2/c^2 - k^2}$. Here, the two-dimensional vectors \mathbf{x} and \mathbf{k} denote the position and momentum vectors parallel to the surface, respectively. Henceforward in this appendix, we use units with $c = \epsilon_0 = 1$. The matrix $R_{\alpha\beta}(\mathbf{k}, \omega)$ is defined as

$$R_{\alpha\beta}(\mathbf{k}, \omega) = (\hat{s}\hat{s})_{\alpha\beta} R^s + (\hat{p}_0+\hat{p}_0-)_{\alpha\beta} R^p \quad (\text{A.2})$$

The functions R^s and R^p in eqn. (A.2) are the Fresnel reflection coefficients for s - and p -polarized light, which can be modeled to realize different surface materials. For the case of a perfectly reflecting surface, $R^s = -1$ and $R^p = 1$, while in general the reflection coefficients are frequency dependent (see [9, 10, 24]): Considering an interface between vacuum ($\epsilon_0 = 1$) and a material with a local and isotropic dielectric function $\epsilon(\omega)$, R^s and R^p are given by

$$R^s = \frac{k_z - (\omega^2 \epsilon(\omega) - k^2)^{1/2}}{k_z + (\omega^2 \epsilon(\omega) - k^2)^{1/2}}, \quad (\text{A.3})$$

$$R^p = \frac{\epsilon k_z - (\omega^2 \epsilon(\omega) - k^2)^{1/2}}{\epsilon k_z + (\omega^2 \epsilon(\omega) - k^2)^{1/2}}. \quad (\text{A.4})$$

In section 5.4, we use the Drude model for a metal surface, with

$$\epsilon(\omega) = 1 - \frac{\omega_p^2}{\omega(\omega + i/\tau)}, \quad (\text{A.5})$$

where ω_p is the plasma frequency and τ the collision time. Finally, the dyadic elements $(\hat{s}\hat{s})_{\alpha\beta}$ and $(\hat{p}_{0+}\hat{p}_{0-})_{\alpha\beta}$ in eqn. (A.2) involve the normalized polarization vectors

$$\hat{\mathbf{s}} = \hat{\mathbf{k}} \times \hat{\mathbf{z}} \quad (\text{A.6})$$

$$\hat{\mathbf{p}}_{0\pm} = \frac{k\hat{\mathbf{z}} \mp k_z\hat{\mathbf{k}}}{\omega}. \quad (\text{A.7})$$

B Approximating the error function integral

In the integrands of eqn. (5.18) and eqn. (6.9), we encounter the expression

$$I(\bar{\kappa}, x, \eta) \equiv \frac{1}{2} \exp[-2\bar{\kappa}x + \bar{\kappa}^2\eta^2] (1 + \operatorname{erf}[\frac{x}{\eta} - \bar{\kappa}\eta]) \quad (\text{B.1})$$

where $\bar{\kappa}$ is integrated from zero to infinity, $\eta = a_0\omega_{eg}/c$ is fixed by the atomic transition frequency and mass and the trap geometry and the positive distance x varies such that $x > \eta^2$ is always fulfilled.

Noting that the argument of the error function changes sign at $\bar{\kappa} = x/\eta$, we can approximate the error function for large values of $\bar{\kappa}$ (see [39, eqn. (8.254)]) to obtain

$$I(\bar{\kappa}, x, \eta) \approx \frac{\exp[-x^2/\eta^2]}{2\sqrt{\pi}(\bar{\kappa}\eta - x/\eta)}, \quad \text{for } \bar{\kappa} \gg \frac{x}{\eta^2} \quad (\text{B.2})$$

which is exponentially small in the quantity $(x/\eta)^2$. In numerical integrations, we will thus cut off the $d\bar{\kappa}$ -integration at $\bar{\kappa} = x/\eta^2$, omitting terms of order $\mathcal{O}(\exp[-(x/\eta)^2])$ in the integrand. The neglected quantities are small: for a rubidium atom at $T = 0$ trapped in a $\nu/2\pi = 1$ kHz trap at an atom-surface distance of $x = d\omega_{eg}/c = 15$, we have $(x/\eta)^2 \approx 30$. Conceptionally, the high momentum cut-off is necessary as the atomic probability density $|\phi_0(\mathbf{r})|^2$ we adopt here is not zero at the surface, but only exponentially small, namely of the same order as the terms neglected in eqn. (B.2).

References

- [1] S. Haroche. Cavity quantum electrodynamics. In J. Dalibard, J.-M. Raimond, and J. Zinn-Justin, editors, *Fundamental Systems in Quantum Optics (Les Houches, Session LIII)*, page 767. North-Holland, 1992.
- [2] E. A. Hinds. Perturbative cavity quantum electrodynamics. In P. R. Berman, editor, *Cavity Quantum Electrodynamics*, Adv. At. Mol. Opt. Phys. Academic, 1994. Suppl. 2.
- [3] H. Bender, Ph. W. Courteille, C. Marzok, C. Zimmermann, and S. Slama. Direct measurement of intermediate-range Casimir-Polder potentials. *Phys. Rev. Lett.*, 104:083201, 2010.
- [4] C. I. Sukenik, M. G. Boshier, D. Cho, V. Sandoghdar, and E. A. Hinds. Measurement of the Casimir-Polder force. *Phys. Rev. Lett.*, 70:560, 1993.
- [5] D. M. Harber, J. M. Obrecht, J. M. McGuirk, and E. A. Cornell. Measurement of the Casimir-Polder force through center-of-mass oscillations of a Bose-Einstein condensate. *Phys. Rev. A*, 72:033610, 2005.
- [6] A. Landragin, J.-Y. Courtois, G. Labeyrie, N. Vansteenkiste, C. I. Westbrook, and A. Aspect. Measurement of the van der Waals force in an atomic mirror. *Phys. Rev. Lett.*, 77:1464, 1996.
- [7] J. M. Obrecht, R. J. Wild, M. Antezza, L. P. Pitaevskii, S. Stringari, and E. A. Cornell. Measurement of the temperature dependence of the Casimir-Polder force. *Phys. Rev. Lett.*, 98:063201, Feb 2007.
- [8] G. Barton and N. S. J. Fawcett. Quantum electromagnetics of an electron near mirrors. *Phys. Rep.*, 170:1, 1988.

- [9] J. M. Wylie and J. E. Sipe. Quantum electrodynamics near an interface. *Phys. Rev. A*, 30(3):1185, 1984.
- [10] J. M. Wylie and J. E. Sipe. Quantum electrodynamics near an interface. II. *Phys. Rev. A*, 32(4):2030, 1985.
- [11] A. L. Fetter and J. D. Walecka. *Quantum Theory of Many Particle Systems*. Dover, 2003.
- [12] M. Lewenstein, L. You, J. Cooper, and K. Burnett. Quantum field theory of atoms interacting with photons: Foundations. *Phys. Rev. A*, 50(3):2207, 1994.
- [13] W. Zhang and D. F. Walls. Quantum field theory of interaction of ultracold atoms with a light wave: Bragg scattering in nonlinear atom optics. *Phys. Rev. A*, 49(5):3799, 1994.
- [14] W. P. Healy. *Non-relativistic quantum electrodynamics*. Academic Press, 1982.
- [15] D. P. Craig and T. Thirunamachandran. *Molecular Quantum Electrodynamics*. Dover, 1998.
- [16] M. P. Gorza and M. Ducloy. Van der Waals interactions between atoms and dispersive surfaces at finite temperature. *Eur. Phys. J. D*, 40:343, 2006.
- [17] S. Weinberg. *The Quantum Theory of Fields*, volume I - Foundations. Cambridge University Press, 2005.
- [18] C. Eberlein and D. Robaschik. Inadequacy of perfect-reflector models in cavity QED for systems with low-frequency excitations. *Phys. Rev. Lett.*, 92(23):233602, 2004.
- [19] C. Eberlein and D. Robaschik. Quantum electrodynamics near a dielectric half-space. *Phys. Rev. D*, 73(2):025009, 2006.
- [20] C. K. Carnaglia and L. Mandel. Quantization of evanescent electromagnetic waves. *Phys. Rev. D*, 3:280, 1971.
- [21] G. S. Agarwal. Quantum electrodynamics in the presence of dielectrics and conductors. I. Electromagnetic-field response functions and black-body fluctuations in finite geometries. *Phys. Rev. A*, 11:230, 1975.
- [22] H. B. Callen and T. A. Welton. Irreversibility and generalized noise. *Phys. Rev.*, 83(1):34, 1951.
- [23] E. A. Hinds and V. Sandoghdar. Cavity QED level shifts of simple atoms. *Phys. Rev. A*, 43(1):398, 1991.
- [24] J. E. Sipe. The dipole antenna problem in surface physics: A new approach. *Surf. Sci.*, 105:489, 1981.
- [25] L. Pitaevskii and S. Stringari. *Bose-Einstein Condensation*. International Series of Monographs on Physics, 116. Clarendon Press, 2003.
- [26] G. L. Klimchitskaya and V. M. Mostepanenko. Conductivity of dielectric and thermal atom-wall interaction. *J. Phys. A: Math. Theor.*, 41(31):312002, 2008.
- [27] V. M. Pérez-García, H. Michinel, J. I. Cirac, M. Lewenstein, and P. Zoller. Dynamics of Bose-Einstein condensates: Variational solutions of the Gross-Pitaevskii equations. *Phys. Rev. A*, 56(2):1424, 1997.
- [28] T. F. Gallagher. *Rydberg atoms*. Cambridge University Press, Cambridge, 1994.
- [29] S. M. Barnett, S. Franke-Arnold, A. S. Arnold, and C. Baxter. Coherence length for a trapped Bose gas. *J. Phys. B: At. Mol. Opt. Phys.*, 33:4177, 2000.
- [30] S. M. Rytov, Y. A. Kravtsov, and V. I. Tatarskii. *Elements of Random Fields*, volume 3 of *Principles of Statistical Radiophysics*. Springer, 1989.
- [31] V. E. Mkrtchian. The force acting on a polarizable nanoparticle in the quantized electromagnetic field. *Armen. J. Phys.*, 1:229, 2009.

- [32] R. Wynar, R. S. Freeland, D. J. Han, C. Ryu, and D. J. Heinzen. Molecules in a Bose-Einstein condensate. *Science*, 287:1016, 2000.
- [33] R. Messina, R. Passante, L. Rizzuto, S. Spagnolo, and R. Vasile. Casimir–polder forces, boundary conditions and fluctuations. *J. Phys. A*, 41:164031, 2008.
- [34] R. Gati, B. Hemmerling, J. Fölling, M. Albiez, and M. K. Oberthaler. Noise thermometry with two weakly coupled Bose-Einstein condensates. *Phys. Rev. Lett.*, 96:130404, 2006.
- [35] S. Hofferberth, I. Lesanovsky, B. Fischer, T. Schumm, and J. Schmiedmayer. Non-equilibrium coherence dynamics in one-dimensional Bose gases. *Nature*, 449(7160):324, 2007.
- [36] C. H. Wu, C. I. Kuo, and L. H. Ford. Fluctuations of the retarded van der Waals force. *Phys. Rev. A*, 65:062102, 2002.
- [37] J. R. Zurita-Sánchez, J. J. Greffet, and L. Novotny. Friction forces arising from fluctuating thermal fields. *Phys. Rev. A*, 69:022902, 2004.
- [38] G. Y. Panasyuk, J. C. Schotland, and V. A. Markel. Short-distance expansion for the electromagnetic half-space Green’s tensor: general results and an application to radiative lifetime computations. *J. Phys. A*, 42:275203, 2009.
- [39] I. S. Gradshteyn and I. M. Ryzhik. *Table of Integrals, Series, and Products*, volume 2. Academic Press Inc., 1980.